

Scanning-tunneling-microscopy-based nanolithography of diamond-like carbon films

Thomas Mühl

Citation: [Applied Physics Letters](#) **85**, 5727 (2004); doi: 10.1063/1.1831567

View online: <http://dx.doi.org/10.1063/1.1831567>

View Table of Contents: <http://scitation.aip.org/content/aip/journal/apl/85/23?ver=pdfcov>

Published by the [AIP Publishing](#)

Articles you may be interested in

[Hydrogen stability in hydrogenated amorphous carbon films with polymer-like and diamond-like structure](#)

J. Appl. Phys. **112**, 093502 (2012); 10.1063/1.4764001

[Cryogenic graphitization of submicrometer grains embedded in nanostructured tetrahedral amorphous carbon films](#)

J. Appl. Phys. **100**, 084319 (2006); 10.1063/1.2360386

[Short-pulse-laser-induced optical damage and fracto-emission of amorphous, diamond-like carbon films](#)

Appl. Phys. Lett. **86**, 121911 (2005); 10.1063/1.1888037

[Deposition and field-emission characterization of electrically conductive nitrogen-doped diamond-like amorphous carbon films](#)

J. Vac. Sci. Technol. A **22**, 1857 (2004); 10.1116/1.1756878

[Fluctuation microscopy studies of medium-range ordering in amorphous diamond-like carbon films](#)

Appl. Phys. Lett. **84**, 2823 (2004); 10.1063/1.1713048

The image shows the cover of the journal Applied Physics Reviews. It features a white background with a blue and orange design. The title 'AIP Applied Physics Reviews' is at the top. Below it is a diagram of a layered structure with labels. The bottom left corner has the URL 'ap.r.aip.org'.

NEW Special Topic Sections

NOW ONLINE
Lithium Niobate Properties and Applications:
Reviews of Emerging Trends

AIP | Applied Physics Reviews

Scanning-tunneling-microscopy-based nanolithography of diamond-like carbon films

Thomas Mühl^{a)}

Leibniz Institute for Solid State and Materials Research Dresden, Helmholtzstrasse 20,
D-01069 Dresden, Germany

(Received 29 April 2004; accepted 11 October 2004)

We demonstrate an approach for nanometer-scale lithography of diamond-like carbon films employing a local electron injection from a scanning tunneling microscope tip under ultrahigh-vacuum conditions. The electrons induce a graphitization of the tetrahedrally bound carbon. With this technique, complex patterns of conducting lines and dots smaller than 10 nm can be written. Tunneling spectroscopy and conductive force microscopy were used to further characterize the carbon nanostructures. © 2004 American Institute of Physics.

[DOI: 10.1063/1.1831567]

Depending on the deposition technology, amorphous carbon films can be prepared with a different ratio of diamond-like (sp^3 -hybridized) to graphite-like (sp^2 -hybridized) bonds. Amorphous carbon films containing a high sp^3/sp^2 ratio are called diamond-like carbon (DLC) films or, more exactly, tetrahedral amorphous carbon (ta-C) films due to a nearly tetrahedral coordination of the carbon atoms as in crystalline diamond. These super-hard ta-C films have high application potential, for example, as wear-resistive coatings of hard disk platters and read/write heads in magnetic data storage technology. Besides the mechanical properties, also the electronic, electrical, optical, and thermal properties of amorphous carbon films depend strongly on their sp^3/sp^2 bond ratio. Therefore, for many applications it is highly desirable to prepare carbon structures with bond types predefined on the nanometer scale. Since in thermodynamic terms sp^3 bonds represent a metastable configuration compared with sp^2 bonds, several approaches addressing this challenge are based on ta-C films, which have to be graphitized within predefined regions by adequate techniques. Seth *et al.* showed that exposure to laser light provides enhanced O_2 plasma etching rates in the exposed regions due to local graphitization.¹ However, laser-based lithographies are limited in spatial resolution. To access the nanometer scale, one can expose DLC films to high-energy ions, which create conducting tracks along their path.^{2,3} Unfortunately, this technique requires expensive high energy equipment. Furthermore, the positions of the conducting tracks are as arbitrary as the ion trajectories are. Strong electric fields applied to metal-contacted DLC films lead to irreversible changes in the I - V characteristics due to the creation of sp^2 islands embedded in the sp^3 matrix.⁴ In order to investigate the effect of high electric fields on ta-C films on a local scale, Mercer *et al.* applied voltage ramps from -10 to $+10$ V using a scanning tunneling microscope (STM) tip in air and in ultrahigh vacuum (UHV).⁵ Spatially resolved electron energy loss spectroscopy measurements indicated an increase of the ratio of sp^2 bonded carbon within the STM treated regions.

In this letter, we demonstrate the huge potential of the STM approach for nanolithography in ta-C films. To shed light onto the sp^3 - sp^2 conversion mechanism, the study also

addresses the dependence of the conversion process on voltage, polarity, current, and ambiance. The modified carbon regions were analyzed by STM based current-distance spectroscopy and by conductive atomic force microscopy (C-AFM).

The ta-C films were prepared on doped Si substrates using the filtered cathodic vacuum arc technique developed by the Fraunhofer-IWS Dresden.⁶ The ta-C films are amorphous with an abundance of sp^3 bonds of about 80%. The STM studies (imaging, patterning, and spectroscopy) were performed in a dedicated UHV system including a scanning electron microscope (SEM) with integrated STM. The pressure during the patterning experiments did not exceed 5×10^{-10} mbar. The SEM enables a controlled coarse positioning of the STM tip with respect to sample features. The SEM maps allow one to find the location of the patterned carbon structures with subsequently employed *ex situ* methods like atomic force microscopy (AFM) and C-AFM. To probe the influence of air, a series of patterning experiments were performed in a second UHV-STM in the vented state.

After introducing the ta-C samples into the STM vacuum chamber, the samples were carefully annealed at 150°C to remove adsorbates. Because of the high resistivity of the ta-C films, the STM was operated in the constant-current mode at relatively high voltage and low current, e.g., 2.6 V and 100 pA, respectively. The conversion process was performed in a software-controlled mode as follows: The tip scanned along the surface under feedback-controlled imaging conditions. At preselected locations, the tip was stopped and the initial voltage V and current I settings were changed to predefined values suitable for local modifications, while the feedback control of the STM was still active. After a certain time period Δt , V and I were reset to the initial values and the tip was moved to the next software-controlled location. These steps were repeated until the process was complete. Immediately after the modification procedure, the modified sample area was imaged using the conventional STM mode.

For local modification in a 30 nm ta-C film as shown in the STM image of Fig. 1, V , I , and Δt were set to -10 V at the tip, 4 nA, and 20 ms, respectively. The total number of dots amounts to 9713 within a 200×200 dot bitmap. As a first observation we note that the film thickness of the modi-

^{a)}Electronic mail: t.muehl@ifw-dresden.de

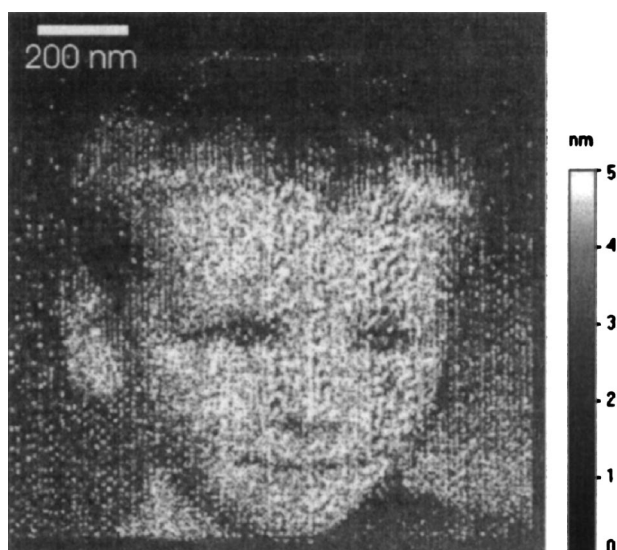


FIG. 1. STM image of a 30-nm-thick ta-C film after electron-induced local modification. The STM parameters during patterning were -10 V, 4 nA, and 20 ms for each dot.

fied sample area seems to be increased by approximately 6 nm. In order to exclude STM-related artifacts, the same sample area was independently measured by AFM, revealing a similar topography image. Both the height and diameter of a dot depend on the patterning parameters V , I , and Δt . Individual dots written using the above-mentioned parameters for Fig. 1 appear in the STM image to have 10 nm in diameter. However, considering the STM tip-sample convolution process, the real dot diameter is likely to be considerably smaller. TEM cross-section studies are under way to clarify this question.

A few STM experiments performed under ambient conditions on the same ta-C samples with the same patterning parameters mentioned earlier lead to the formation of holes and trenches in the ta-C film which can be related to a local electron-induced oxidation of the carbon, which is in agreement with our previous results.^{7,8} However, Mercer *et al.* did not find any influence of the ambient environment.⁵

To study the influence of V and I on the patterning process, square-shaped 100 nm areas were scanned with V or I varied from square to square. For positive tip voltages up to 10 V, no modification could be observed. Negative tip voltages above a threshold of around 4 V lead to a local increase Δd of the film thickness (Fig. 2). Both the $\Delta d(V)$ relation and

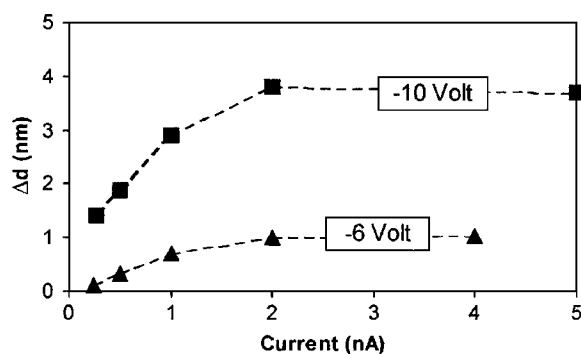


FIG. 2. Current dependence of the local film thickness increase Δd of a 20 -nm-thick ta-C film for -6 and -10 V. Each data point corresponds to a square-shaped sample area which was modified by scanning for 50 s.

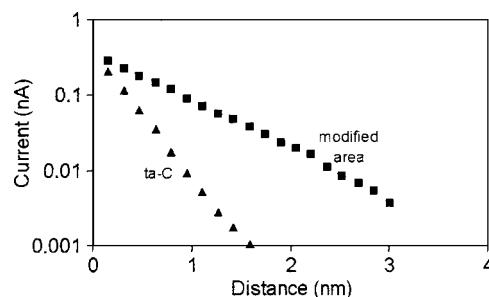


FIG. 3. STM-based current-distance curves of the STM-modified vs the original ta-C film measured with a constant tip voltage of -2.46 V.

the $\Delta d(I)$ relation seem to be nonlinear and depend on the ta-C film thickness. Δd saturates at high current values. The Δd maximum is voltage dependent.

The observed increase of film thickness (positive Δd) can be explained by a local decrease of the carbon density due to a local graphitization. We can tentatively conclude this graphitization which is related to a sp^3 to sp^2 bond change, on the basis of the following findings: Compared with the original ta-C film, the modified sample areas show (i) a density decrease, (ii) a decrease of the tunneling barrier height, (iii) a strongly increased electrical conductivity, and (iv) changes in the secondary electron emission rate. (ii)–(iv) will be presented in the following sections.

After the local graphitization in the UHV-STM, both the modified areas and the original ta-C film were investigated by STM-based current-distance spectroscopy (Fig. 3). For the STM-modified sample areas there is a much lower decrease in current with distance than for the original ta-C film. This can be related to a reduced tunneling-barrier height. Since we can safely assume that the tungsten STM tip properties do not change, the observation can be associated with the electronic properties of the carbon film being different in the modified areas and the original film, respectively. In particular, the work function of the modified region seems to be reduced. The data of Fig. 3 can be fitted by an exponential decay function. The decay constants amount to 3.7 and 1.4 nm $^{-1}$ for the original ta-C film and for the STM-modified sample area, respectively.

For local conductivity measurements by means of C-AFM, Pt–Ir coated Si probes were used in contact mode. The current image of a 20 nm ta-C film after the STM-based structuring of line-shaped patterns is shown in Fig. 4. The lines sustain more than 2 nA, while the unmodified regions are almost insulating. Not all of the STM-written patterns show such a clear current contrast in C-AFM. Although all UHV-STM written patterns in the ta-C films investigated in this study exhibit a film thickness increase and a tunneling barrier decrease, it was difficult to get current images in the case of samples with a ta-C thickness of more than 25 nm. Probably, the depth of the STM-induced graphitization region did not reach through the entire film thickness and therefore the graphitized islands were not electrically connected to the doped-Si substrate. According to preliminary SEM experiments, the secondary electron emission characteristic seems to be related to the electrical connection to the substrate: The secondary electron emission of the conducting structures in Fig. 4 is reduced, but it is increased for the carbon nanostructures in thicker films without electrical connection to the substrate.

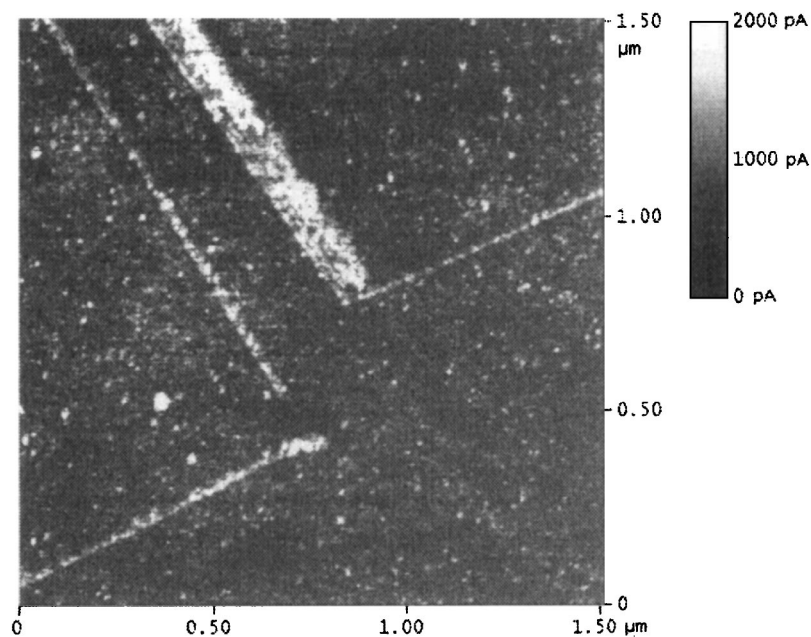


FIG. 4. C-AFM image of a 20-nm-thick ta-C film after electron-induced local modification along three single and a bundle of parallel lines. A sample bias of -900 mV was applied. Only in the modified regions a sizeable current gives rise to the image contrast.

Even though there is no full understanding of the microscopic mechanism of the STM induced local graphitization, the experimental results indicate that field-emitted free electrons enter the ta-C film and are absorbed within the film. The efficiency of the impinging electron beam for the local ta-C modification depends strongly on the electron energy which is related to the STM tip voltage. For example, as shown in Fig. 2, for a 2 nA current the local film thickness increase, Δd , with -10 V is nearly four times larger than in the -6 V case. The understanding of the lower Δd saturation value in the -6 V case is not straightforward. Possibly there is a space charge induced potential drop within the highly resistive ta-C.

In contrast, local Joule heating due to the introduced power as the main reason for the graphitization can be ruled out because of the fact that two experiments with the same power injection but different voltage (e.g., -10 V, 1 nA vs -5 V, 2 nA) lead to quite different patterning results.

The results presented in this study support the interpretation that the STM tip electron emission in ta-C films induces nano-sized areas with increased sp^2 content. There are a lot of possible applications of these graphitic nanostructures within an insulating ta-C matrix: Dots for high density data storage with long-term stability, conducting one-

dimensional lines for nano-electronics, etching masks for further nano-lithography steps, etc.

The author thanks B. Schultrich, V. Weihnacht, and P. Siemroth from the Fraunhofer-IWS Dresden for providing the ta-C samples and for many discussions. Additional helpful discussions with I. Mönch, J. Schumann, S. Zotova, S. Baunack, T. Gemming, A. Winkler, M. Rummeli, C. M. Schneider, K. Mühl, and A. Biella are gratefully acknowledged.

- ¹J. Seth, S. V. Babu, V. G. Ralchenko, T. V. Kononenko, V. P. Ageev, and V. E. Strel'nitsky, *Thin Solid Films* **254**, 92 (1995).
- ²J.-H. Zollondz, J. Krauser, A. Weidinger, C. Trautmann, D. Schwen, C. Ronning, H. Hofsaess, and B. Schultrich, *Diamond Relat. Mater.* **12**, 938 (2003).
- ³J. Krauser, J.-H. Zollondz, A. Weidinger, and C. Trautmann, *J. Appl. Phys.* **94**, 1959 (2003).
- ⁴C. Ronning, U. Griesmeier, M. Gross, H. C. Hofsaess, R. G. Downing, and G. P. Lamaze, *Diamond Relat. Mater.* **4**, 666 (1995).
- ⁵T. W. Mercer, N. J. DiNardo, J. B. Rothman, M. P. Siegal, T. A. Friedmann, and L. J. Martinez-Miranda, *Appl. Phys. Lett.* **72**, 2244 (1998).
- ⁶P. Siemroth and T. Witke, *IEEE Trans. Plasma Sci.* **27**, 1039 (1999).
- ⁷T. Mühl, H. Brückl, G. Weise, and G. Reiss, *J. Appl. Phys.* **82**, 5255 (1997).
- ⁸T. Mühl, J. Kretz, I. Mönch, C. M. Schneider, H. Brückl, and G. Reiss, *Appl. Phys. Lett.* **76**, 786 (2000).